ISSN 0965-545X, Polymer Science, Series A, 2018, Vol. 60, No. 1, pp. 65–73. © Pleiades Publishing, Ltd., 2018.
Original Russian Text © S.A. Vshivkov, E.V. Rusinova, 2018, published in Vysokomolekulyarnye Soedineniya, Seriya A, 2018, Vol. 60, No. 1, pp. 66–75.

NATURAL POLYMERS

Effect of Component Nature on Liquid-Crystalline Transitions in Solutions of Cellulose Ethers

S. A. Vshivkov* and E. V. Rusinova

Ural Federal University, pr. Lenina 51, Yekaterinburg, 620000 Russia

**e-mail: sergey.vshivkov@urfu.ru*

Received December 12, 2016;
Revised Manuscript Received May 22, 2017

Abstract—The experimental data on phase liquid-crystalline transitions in solutions of cellulose ethers are summarized. The effect of polymer molecular mass, the rise of which leads to the shift of boundary curves to the regions of higher temperatures and lower polymer concentrations, is considered. The replacement of the hydroxypropyl radical in cellulose ether units by the ethyl or hydroxyethyl radical leads to a decrease in the concentration of the LC phase. It is shown that the higher the polarity of solvent molecules, the more negative the Gibbs energy of mixing and the higher the second virial coefficients, i.e., the better the solubility of cellulose ethers.

DOI: 10.1134/S0965545X18010078

INTRODUCTION

Liquid crystals play a great role in science and engineering [1–10]. A high self-organizing ability of these compounds is of significant interest for designing of new materials. V.A. Kargin was the first to indicate the ability of polymers to form mesophases in 1941: "... interactions between large molecules will be quite significant even at a rather weak interaction of individual units. This ... can lead to the orientation of such large molecules in a certain common direction ..." [11]. The LC state in the solutions and melts of cellulose derivatives was discovered and studied in the 1970s–1980s [1, 12–27]. The molecules of cellulose and its derivatives have rigid helical conformations in the ordered regions which are stabilized by intramolecular hydrogen bonds. If dissolution of these polymers is not accompanied by the breakage of intramolecular H bonds, then the molecules remain rigid-chain and, consequently, they are capable of ordering and formation of liquid crystals of the cholesteric type. If dissolution leads to the breakage of intramolecular H bonds, then chains become flexible and, as a result, stop ordering. Therefore, in order to obtain the LC state of the solutions of cellulose and its derivatives, solvents breaking only intramolecular H bonds (DMF, DMAA, 1,4-dioxane, chlorinated hydrocarbons) are used. The phase diagrams of cellulose derivative solutions were constructed for cellulose tricarbanilate–methyl ethyl ketone, oxypropyl cellulose–water, hydroxypropyl cellulose–DMAA, hydroxypropyl cellulose–ethanol, hydroxypropyl cellulose–acetic acid, hydroxypropyl cellulose–DMAA, cyanoethyl cellulose–DMAA, hydroxyethyl cellulose–DMF, and hydroxyethyl cellulose–water systems [12–14, 28–36].

The thermodynamic properties of cellulose ether solutions were investigated [37–39]. For example, the formation of the LC mesophase by cyanoethyl hydroxyethyl cellulose in some organic solvents were considered in [37] and a difference in the mechanisms of structural rearrangement of the systems during the process of solvent sorption was found. A linear change in the enthalpy, entropy, and Gibbs energy of mixing in the region of anisotropic cholesteric mesophase for hydroxypropyl cellulose solutions in water and ethanol was observed in [39].

However, no data are available on the generalization and analysis of the effect of the chemical structure of cellulose ether molecules and solvents on phase transitions. Therefore, the present work is aimed at gaining insight into the effect of the nature of components on LC transitions using both new and previously published experimental data.

EXPERIMENTAL

The objects of this study were hydroxypropyl cellulose (HPC) of the Klucel-JF trademark (Hercules, United States); cyanoethyl cellulose (CEC), cyanoethyl nitrocellulose (CENC), cyanoethyl hydroxyethyl cellulose (CEHEC), and methyl cellulose (MC) (Institute of Macromolecular Compounds, Russian Academy of Sciences, Russia); and

Table 1. Characteristics of research objects

Cellulose ether	Molecular mass	Degree of substitution, α
HPC-1	$M_w = 0.9 \times 10^5$	3.0
HPC-2	$M_w = 1.5 \times 10^5$	3.3
HPC-3	$M_\eta = 4.5 \times 10^5$	3.0
HPC-4	$M_w = 1.15 \times 10^6$	3.0
CEC	$M_w = 0.90 \times 10^5$	2.6
HEC-1	$M_w = 6.2 \times 10^4$	2.5
HEC-2	$M_w = 8.6 \times 10^4$	2.5
HEC-3	$M_\eta = 1.0 \times 10^5$	2.5
HEC-4	$M_\eta = 4.5 \times 10^5$	2.5
EC-1	$M_\eta = 2.6 \times 10^4$	2.6
EC-2	$M_w = 1.6 \times 10^5$	1.5
CENC	$[\eta] = 2.79$ dL/g (DMAA, $T = 298$ K)	0.19
MC	$M_\eta = 1.8 \times 10^5$	2.0
CEHEC	$M_\eta = 10^5$	2.0

hydroxyethyl cellulose (HEC) and ethyl cellulose (EC) (Hercules–Aqualon and ACROS–USA). Their characteristics are presented in Table 1.

DMF, DMAA, ethanol, bidistilled water, acetic acid (glacial), and TFAA–methylene chloride mixture (1 : 1 ratio) were used as solvents. The purity of solvents was controlled via refractometry. Polymer solutions were prepared in sealed ampoules for several weeks at 298 K in water, 330 K in ethanol, and 350 K in DMF, DMAA, acetic acid, and TFAA–methylene chloride. The phase transition temperature T_{ph} in polymer solutions was determined by the method of cloud points [40]. The rate of cooling (heating) of the solutions was 0.2 K/min. The temperature corresponding to the onset of solution turbidity was taken as the phase-transition temperature. The error of T_{ph} determination by this method was ±0.2 K. The observed phenomenon was reversible. The phase state of the systems was studied on an Olympus BX-51 polarizing microscope. The type of phase transition in the solutions was determined using a polarization-photovoltaic setup [40]. A sealed ampoule with the transparent polymer solution was placed in a gap between the crossed polaroids (polarizer and analyzer), and the temperature was decreased using a thermostatic jacket. The light beam of a helium-neon laser was passed through the polaroids perpendicularly to the ampoule with the solution (the solution layer thickness was ~5 mm). When the solution became transparent (isotropic), the intensity of the light passing through the crossed polaroids equaled zero. The system turbidity caused by a change in temperature or a rise in solution concentration led to an increase in the intensity of light transmission registered by a photoresistor. This indicated the anisotropic character of the formed phase, that is, the phase LC transition. The temperature corresponding to the onset of transmitted light intensity was taken as the temperature of formation of the LC phase.

RESULTS AND DISCUSSION

Effect of Polymer Molecular Mass on Phase LC Transitions in Cellulose Ether–Solvent Systems

According to the Flory theory [41], the critical volume fraction of a polymer at which the LC phase is formed in the system is related to the asymmetry of a macromolecule x via the equation $\varphi_2^* = (1 - 2/x)8/x$, where φ_2^* is the critical volume fraction of the polymer and x is the degree of asymmetry of the macromolecule (the length-to-diameter ratio of the molecule). The dilute solutions of HPC in ethanol were studied by light scattering [42]. It was found that HPC in ethanol is dispersed into individual macromolecules with $M = 1.6 \times 10^5$ and a radius of gyration of 74 nm. The authors assumed that the macromolecules are asymmetrical and oblong in shape. The greater the molecular mass and the sizes of the macromolecule, the higher the asymmetry and the higher the x and the lower the φ_2^*.

Figure 1 shows the boundary curves for the HPC-1–DMAA, HPC-3–DMAA, HPC-1–ethanol, HPC-2–ethanol, HPC-3–ethanol, HEC-1–water, and HEC-3–water systems. These curves separate transparent isotropic solutions (I) from opalescent anisotropic solutions (II) (ω_2 is the mass fraction of the polymer in solution).

As follows from the above data, a rise in polymer molecular mass leads to a shift of the boundary curve separating the isotropic and anisotropic regions to the region of lower concentrations, in agreement with the Flory theory. Thus, the systems with LC transitions follow the same dependence as systems with crystalline phase separation [45]; i.e., with a rise in the molecular mass of the crystallizing polymer, the liquidus curve also shifts to lower polymer concentrations and higher temperatures. It should be noted that the Flory theory does not consider influence of the chemical structure of polymer and solvent molecules on phase LC transitions.

Effect of the Chemical Structure of Polymer Molecules on Phase LC Transitions

Figure 2 illustrates the data on phase transitions for the HPC-1–DMF and EC-1–DMF systems. It is

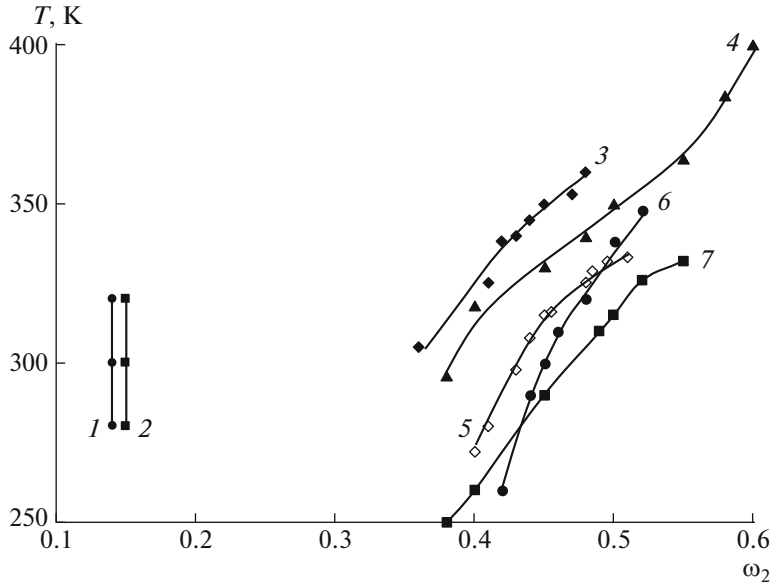

Fig. 1. Boundary curves of (*1*) HEC-4 ($M_\eta = 4.5 \times 10^5$)–water, (*2*) HEC-1 ($M_w = 6.2 \times 10^4$)–water, (*3*) HPC-4 ($M_w = 1.15 \times 10^6$)–ethanol, (*4*) HPC-2 ($M_w = 1.5 \times 10^5$)–ethanol, (*5*) HPC-4 ($M_w = 1.15 \times 10^6$)–DMAA, (*6*) HPC-1 ($M_w = 0.9 \times 10^5$)–ethanol, and (*7*) HPC-1 ($M_w = 0.9 \times 10^5$)–DMAA systems.

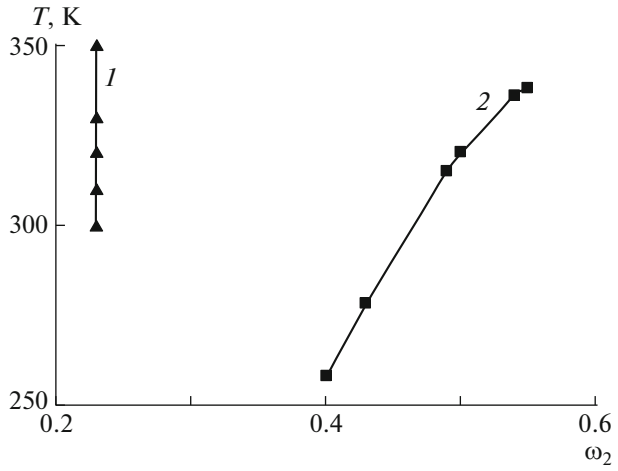

Fig. 2. Boundary curves of (*1*) EC-1($M_\eta = 2.6 \times 10^4$)–DMF and (*2*) HPC-1($M_w = 0.9 \times 10^5$)–DMF systems.

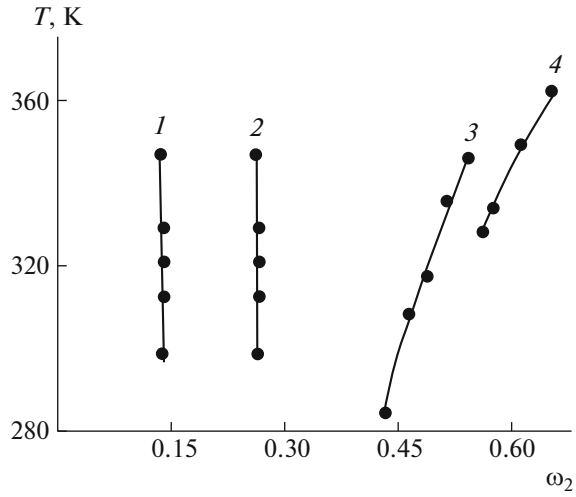

Fig. 3. Boundary curves of (*1*) EC-1($M_\eta = 2.6 \times 10^4$)–ethanol, (*2*) EC-1($M_\eta = 2.6 \times 10^4$)–DMF, (*3*) HPC-2 ($M_w = 1.5 \times 10^5$)–ethanol, and (*4*) HPC-2 ($M_w = 1.5 \times 10^5$)–DMSO systems.

seen that the boundary curve of the EC-1–DMF system separating the isotropic solutions from anisotropic ones is in the region of lower polymer concentrations than the boundary curve of the HPC-1–DMF system. Replacing the branched hydroxylpropyl radical with the ethyl radical enhances interaction between the units of neighboring macromolecules of the EC polymer, thereby facilitating formation of the LC phase. At the same time, a lower polarity of EC-1 molecules worsens interaction with the polar DMF solvent.

Figure 3 shows the boundary curves of the EC-1–ethanol, EC-1–DMF, HPC–ethanol, and HPC-2–DMSO systems. From the above data, it follows that, as for DMF solutions in Fig. 2, in the case of ethanol solutions the replacement of the hydroxypropyl radical with the ethyl radical in cellulose ether units leads to a decrease in the concentration of formation of the LC

Table 2. Diameters d_w of light-scattering particles and mean-square distances between chain ends $(h^2)^{1/2}$ of cellulose ether macromolecules, $T = 298$ K [46]

System ($\omega_2 = 0.05$)	d_w, nm	$(h^2)^{1/2}$, nm
CEC–DMAA	110	60
CEC–DMF	300	60
HPC-1–ethanol	320	64
HPC-1–water	180	64
HEC-1–water	1780	45
HEC-1–DMF	2480	45
HEC-2–DMF	1600	51
HEC-2–DMAA	1800	51
EC-2–DMAA	580	80

phase. A similar dependence is observed for the EC-1–DMF and HPC-2–DMSO systems.

The boundary curves separating the isotropic solutions from anisotropic ones for the HPC–ethanol, HPC–DMAA, and HPC–DMSO systems change with temperature (Figs. 1–3). This is probably caused by the fact that at high temperatures the thermal motion of the molecules can disturb the liquid-crystalline order. Consequently, a high concentration of the polymer is required to retain the liquid-crystalline order.

The boundary curves of the HEC–water (Fig. 1), EC–DMF, and EC–ethanol systems (Fig. 3) do not depend on temperature and are located in the region of lower concentrations. This can be explained by a strong interchain interaction and a higher packing density of EC and HPC macromolecules. Indeed, the linear ethyl and hydroxyethyl radicals in the units of neighboring EC and HEC macromolecules can produce a denser packing with each other than the branched propyl radicals of HPC [43, 44].

For example, the IR study of cellulose ether films showed that the absorption band due to the stretching vibrations of hydroxyl groups ν_{OH} is shifted to lower wavenumbers relative to the absorption band due to the stretching vibrations of O–H bonds of hydroxyl groups in the absence of intermolecular interactions [45]. This shift is caused by the formation of intra- and intermolecular hydrogen bonds with different strengths. The absorption band for HEC is shifted to lower frequencies compared with the bands of CEC and CEHEC. This shift suggests the weakening of O–H bonds due to formation of hydrogen bonds between hydroxyl groups of a macromolecule and hydroxyl groups and oxygen atoms of neighboring macromolecules. Consequently, HEC is a more associated polymer than CEC and CEHEC. For CEC, the absorption band due to O–H groups is observed in a higher frequency region. Hence, it is a less associated compound. CEHEC occupies the intermediate position. Methyl cellulose is also associated but to a lesser extent. This is caused by the presence of the methoxy group in chain units, which decreases the fraction of hydrogen bonds between macromolecules.

As a result of a stronger interchain interaction between EC and HEC macromolecules, large supramolecular particles are formed in their solutions which do not decompose under heating. This is confirmed by the data on diameters of supramolecular particles d_w of EC and HEC (Table 2 [46]). The value of $d_w = 2r_w$, where r_w is the weight-average radius of particles scattering light, as determined by the turbidity spectrum method. Therefore, the position of the boundary curves for the EC–DMF and EC–ethanol systems does not depend on temperature.

A comparison of the values of d_w and the sizes of macromolecules $(h^2)^{1/2}$ (Table 2) shows that, at a mass fraction of the polymer of $\omega_2 = 0.05$, light-scattering particles are supramolecular, For the CEC and HPC solutions, the diameters of light-scattering particles do not exceed 320 nm, for the EC solutions, they are 580 nm; and for the HEC solutions, they vary from 1600 to 2480 nm. The light-scattering particles of HPC and CEC consist of several macromolecules. The molecular-disperse solutions are not formed in the systems based on HEC and EC. Coarse light-scattering particles are probably the residues of the initial structure of the polymer stabilized by a great amount of strong hydrogen bonds formed between neighboring hydroxyl groups and a denser packing of linear ethyl and hydroxyethyl radicals in the units of neighboring macromolecules.

Figure 4 illustrates the boundary curves of the CENC–DMAA, CENC–DMF, CEC–DMF, and CEC–DMAA systems. It is seen that, in the CENC solutions, the LC order appears at a lower concentration of the polymer. This can be connected with the fact that the introduction of a nitro group into CEC chain units increases the rigidity of chains; as a result, the degree of asymmetry of macromolecules grows and, consequently, the LC phase is formed at lower concentrations of the polymer.

The boundary curves for the aqueous solutions of HPC-1 and HEC-1 are given in Fig. 5. It is clear that the replacement of the hydroxypropyl radical in macromolecules with the hydroxyethyl one leads to a substantial change in the phase diagram: first, the LC phase in HEC solutions is formed at lower concentrations. This can be attributed to the linear character and a smaller size of the hydroxyethyl radical compared with the hydroxypropyl one. As a consequence, interchain interaction is enhanced. Secondly, the LCST is absent in the HEC solutions. HPC contains 10–15% of the crystalline phase and 90–85% of the vitrified cholesteric LC phase [24, 25]. The degree of crystal-

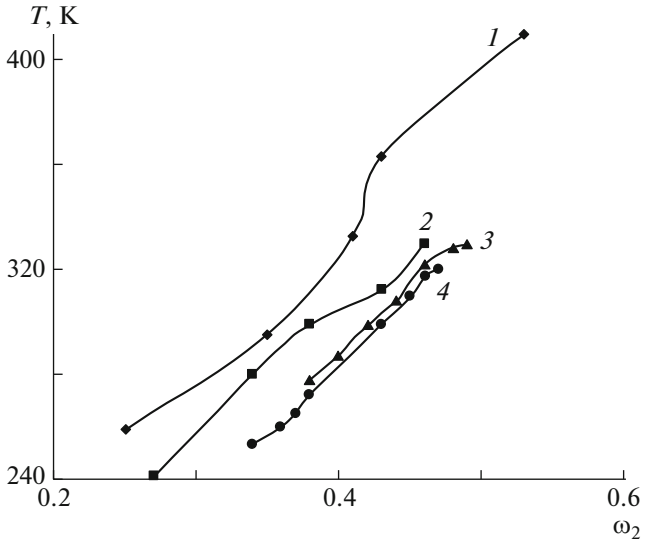

Fig. 4. Boundary curves of (*1*) CENC–DMAA, (*2*) CENC–DMF, (*3*) CEC ($M_w = 0.9 \times 10^5$)–DMF, and (*4*) CEC ($M_w = 0.9 \times 10^5$)–DMAA systems.

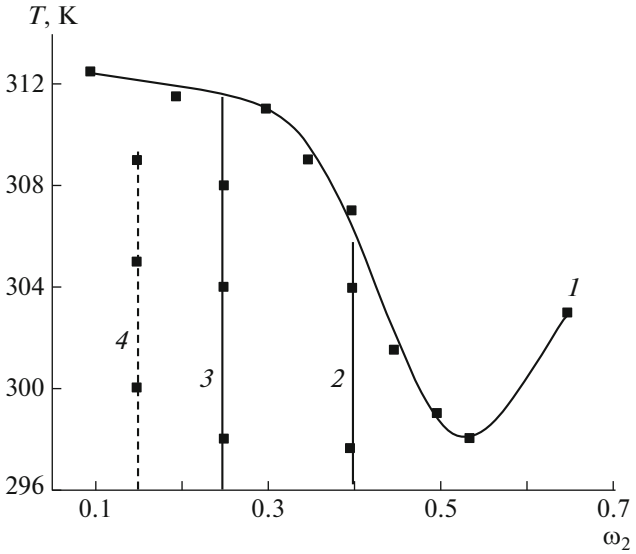

Fig. 5. Boundary curves of (*1–3*) HPC-1($M_w = 0.9 \times 10^5$)–water and (*4*) HEC-1($M_w = 6.2 \times 10^4$)–water systems. Curves *3* and *4* are the boundaries of the isotropic–anisotropic solution transition, and curves *2* and *3* restrict the region of coexistence of isotropic and anisotropic phases.

linity of HEC is almost zero. In the case of HPC, structural changes during dissolution in water may be attributed to the isothermal melting of crystalline domains and relaxation of the metastable glasslike structure. For HEC, only relaxation of the metastable glasslike structure may be observed.

The intermolecular interactions of HPC with water are determined both by the solvation of macromolecules by water accompanied by the formation of hydrogen bonds between a polymer and a solvent [1, 47] and the "hydrophobic hydration" of water itself [48]. The latter process includes the compaction of water structure during penetration of nonpolar molecules or their fragments into voids in its structure. In the case of HPC, methyl and methylene groups of the polymer may be nonpolar fragments. As a result, intermolecular distances in water decrease, the interaction between its molecules becomes stronger, the exothermic effect of dissolution grows, and the entropy of mixing decreases owing to additional structuring [39]. It seems likely that the interactions of both types contribute to the negative enthalpy and entropy of mixing of HPC with water. In accordance with [26], phase separation of the HPC–water system with increasing temperature may be explained by the temperature melting of the densified water structure around hydrophobic fragments of the polymer. The intermolecular interactions of HEC with water can also be determined both by the solvation of macromolecules by water accompanied by the formation of hydrogen bonds between the polymer and solvent and by the "hydrophobic hydration" of water itself. However, since there are no methyl groups in HEC molecules, the "hydrophobic hydration" manifests itself to a lesser extent and the LCST is absent for this system.

Figure 6 shows the boundary curves of the HEC-2–DMAA, EC–DMAA, and HPC-1–DMAA systems. It is seen that the solutions of HEC, EC, and HPC in DMAA follow the same shift in the boundary curves as water and ethanol solutions because of the reasons described above. The replacement of the hydroxyethyl radical in HEC with the ethyl radical in EC leads to the weakening of interchain interactions

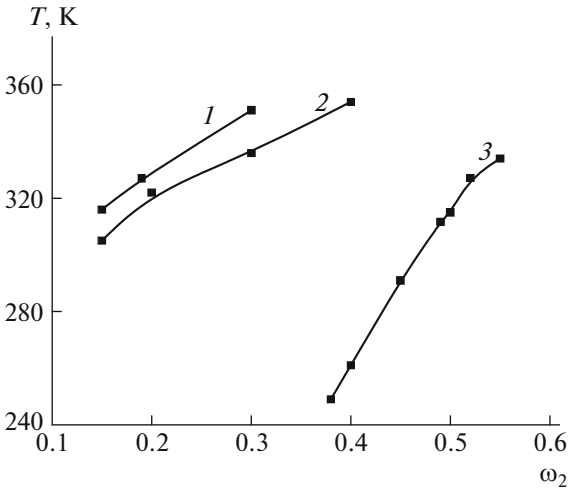

Fig. 6. Boundary curves of (*1*) HEC-2 ($M_w = 8.6 \times 10^4$)–DMAA, (*2*) EC-2 ($M_w = 1.6 \times 10^5$)–DMAA, and (*3*) HPC-1 ($M_w = 0.9 \times 10^5$)–DMAA systems.

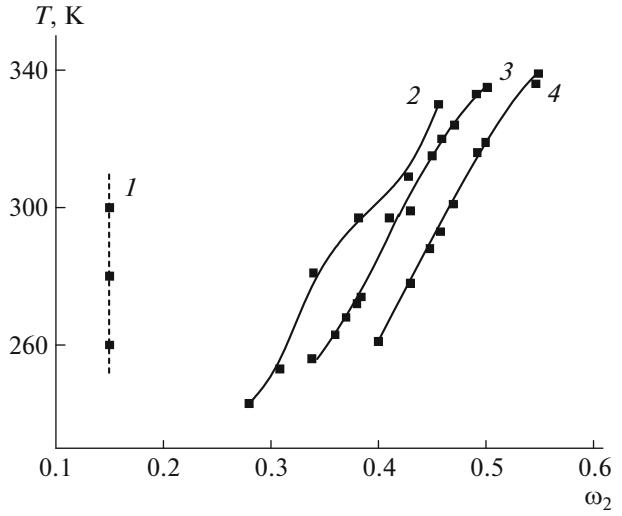

Fig. 7. Boundary curves of (*1*) HEC-1 ($M_w = 6.2 \times 10^4$)–DMF, (*2*) CENC–DMF, (*3*) CEC ($M_w = 0.9 \times 10^5$)–DMF, and (*4*) HPC-1 ($M_w = 0.9 \times 10^5$)–DMF systems.

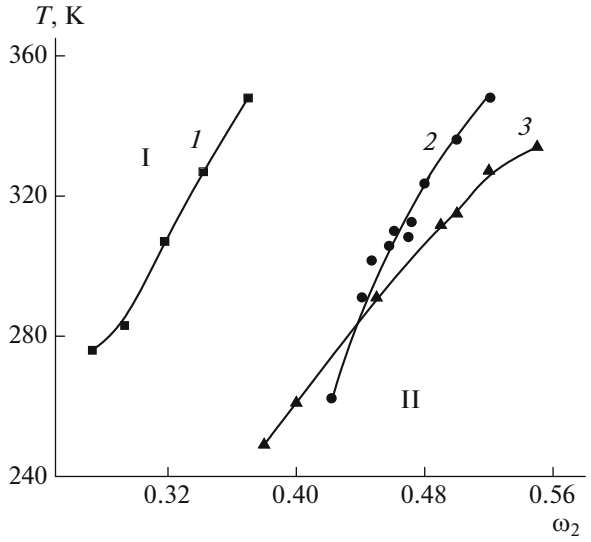

Fig. 8. Boundary curves of (*1*) HPC-1 ($M_w = 0.9 \times 10^5$)–acetic acid, (*2*) HPC-1 ($M_w = 0.9 \times 10^5$)–ethanol, and (*3*) HPC-1 ($M_w = 0.9 \times 10^5$)–DMAA systems. Here and in Figs. 9 and 10, I refers to the region of isotropic solutions, and II refers to the region of anisotropic solutions.

owing to a decrease in the possible formation of hydrogen bonds and, as a result, owing to a rise in concentration of LC phase formation. Note that the boundary curves for the solutions of HEC and EC are in the region of lower concentrations than the solutions of HPC. This is connected with the presence of bulky branched hydroxypropyl radicals in HPC molecules.

The boundary curves for the HEC-1–DMF, CENC–DMF, CEC–DMF, and HPC-1–DMF systems are presented in Fig. 7. For the solutions of these polymers in DMF, the same regularities as for the solutions in DMAA are observed.

Effect of the Chemical Structure of Solvent Molecules on Phase LC Transitions

Figures 8–10 illustrate the boundary curves for HPC and CEC solutions in different solvents. It is seen that the position of the boundary curves on the composition significantly depends on the solvent nature. The better the solvent, to a lesser degree it deteriorates the initial structure of the polymer. Therefore, the LC phase in solution will form at a higher polymer content. A more polar solvent should be better for polar cellulose ethers. Table 3 compares the second virial coefficients and dipole moments of solvent molecules for cellulose acetate solutions.

As follows from Table 3, an increase in the polarity of solvent molecules entails a rise in second virial coefficients, suggesting the improvement of thermodynamic interaction of the components.

As is seen from Fig. 3, the boundary curve of the HPC-2–ethanol system is in the region of lower concentrations than the curve of the HPC-2–DMSO system. This can also be connected with different polarities of solvent molecules. The dipole moment of ethanol molecules $\mu = 1.69$ D [50] is lower than the dipole moment of DMSO $\mu = 3.96$ D [50]. A more polar solvent DMSO deteriorates the initial structure of the polar polymer to a greater extent; as a consequence, the sizes of supramolecular particles decrease. There-

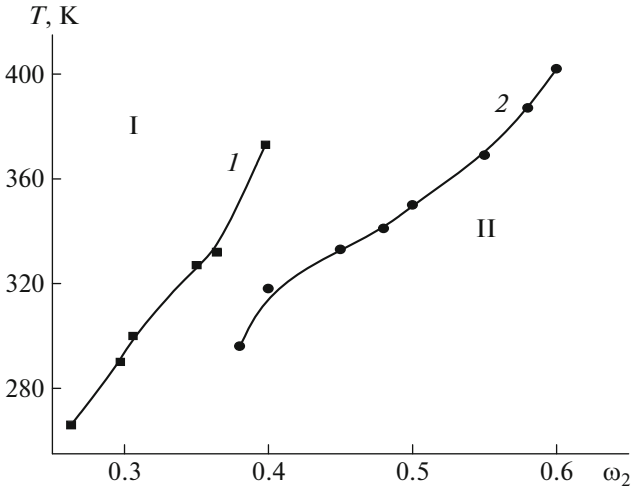

Fig. 9. Boundary curves of (*1*) HPC-2 ($M_w = 1.5 \times 10^5$)–acetic acid and (*2*) HPC-2 ($M_w = 1.5 \times 10^5$)–ethanol systems.

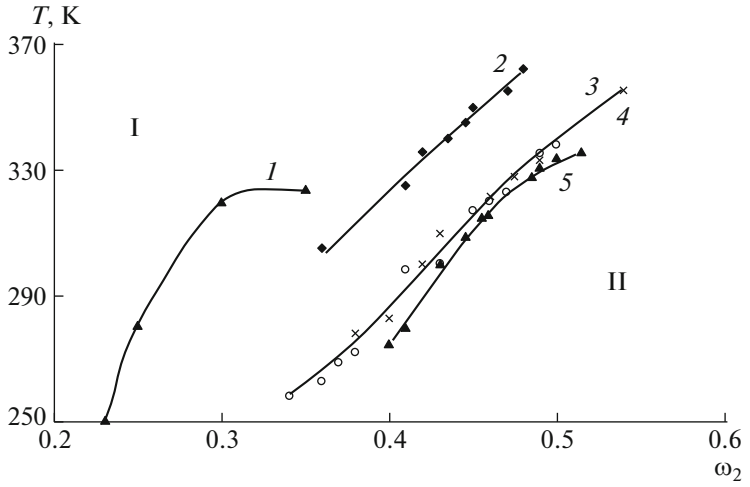

Fig. 10. Boundary curves of (*1*) CEC ($M_w = 0.9 \times 10^5$)–TFAA/MEC, (*2*) HPC-4 ($M_w = 1.15 \times 10^6$)–ethanol, (*3*, light circles) CEC ($M_w = 0.9 \times 10^5$)–DMF, (*4*) CEC ($M_w = 0.9 \times 10^5$)–DMAA, and (*5*) HPC-4 ($M_w = 1.15 \times 10^6$)–DMAA systems.

fore, a high concentration of polymer is needed for formation of the LC order in solutions. A similar dependence is observed for the EC solutions. The dipole moment of DMF molecules μ = 3.81 D [50] is higher than the dipole moment of ethanol molecules μ = 1.69 D and the LC state forms in the EC–DMF system at a higher polymer concentration.

Table 3. Second virial coefficients and dipole moments of solvent molecules for cellulose acetate solutions [49]

Solvent	$A_2 \times 10^4$ cm^3 mol/g^2	Dipole moment, D
DMAA	7.5	3.86
Water	3.1	1.68
Formamide	8.4	3.7

Table 4. Dipole moments and minimum Gibbs energies of mixing of cellulose ethers with low-molecular-mass liquids

Polymer	Solvent	μ, D [51]	$-\Delta g^m$, J/mol solution [45]
MC	Chloroform	1.06	1400
	H_2O	1.83	1350
	Ethanol	1.69	1200
CEC	Chloroform	1.06	1400
	H_2O	1.83	1250
	Acetone	2.85	1400
	Ethanol	1.68	900
CEHEC	Chloroform	1.06	1400
	TFAA	2.28	4250
	H_2O	1.83	1150
	Dioxane	0.45	1250
	Acetone	2.85	1700
HEC	Chloroform	1.06	1300
	H_2O	1.83	1700
	Ethanol	1.68	1050
	Dioxane	0.45	300

Table 4 compares the thermodynamic parameters of interaction for the cellulose ether–solvent systems and the physical properties of the solvents [45, 51]. The thermodynamic parameters for water solutions of the polymers are different. The dissolving capacity of water is provided by the possibility to form hydrogen bonds between its molecules and molecules of other compounds. For HEC containing the maximal amount of hydroxyl groups, water is the best solvent. Almost the same good interaction with chloroform and water is characteristic of MC, the least associated polymer with a small nonpolar substituent and unsubstituted hydroxyl groups.

At the same time, CEC and CEHEC containing polar nitrile groups with donor properties [51] have a high affinity for chloroform and a low affinity for water despite the presence of unsubstituted hydroxyl groups. Owing to a high packing density and, as a result, strong interchain interaction, CEC does not dissolve but only limitedly swells in water. This may suggest an insignificant role of hydrogen bonds in dissolving cyanoethylated ethers. This assumption is confirmed by a low affinity of CEC for ethanol. Dioxane being the electron donor for polymer molecules [51] capable of H bonding has a low thermodynamic affinity for HEC and CEHEC. As follows from Table 4, with some exceptions, the higher the polarity of solvent molecules (the higher the dipole moment of molecules), the more negative the Gibbs energy of mixing, i.e., the better the solubility of the cellulose ethers under investigation. Thus, in a first approximation, the dipole moment may be used as an estimate of solvent quality for cellulose ethers.

Table 5. Dipole moment, ionization potential, acceptor numbers of solvents, and concentrations of LC phase formation in systems, $T = 298$ K

Solvent	μ, D [50, 51]	φ, eV [52]	A [51, 52]	ω_2^*			
				HPC-1	HPC-2	HPC-4	CEC
DMAA	3.86	≤9.65	13.6	0.45	–	0.43	0.42
DMF	3.81	≤10.16	16.0	–	–	–	0.42
Ethanol	1.69	10.25	37.1	0.44	0.38	<0.36	Limitedly swells
Acetic acid	1.74	10.35	52.9	0.3	0.305	–	–
Water	1.84	12.59	54.8	0.25	0.25	0.195	Limitedly swells

Nevertheless, it is known that the molecules of cellulose and its derivatives interact with each other via hydrogen bonds and the solvent should form stronger hydrogen bonds with cellulose ether molecules. In other words, the solvent should also be quite a good donor of electrons, as confirmed by the data of Table 5 [46].

The polarity of solvent molecules was characterized by the dipole moment and the ability to donate electrons was characterized by the ionization potential and the acceptor numbers. It is clear that the lower the ionization potential and, consequently, the higher the polarization capacity and the ability to donate electrons, the higher the polymer concentration at which the LC phase is formed in the system and, thus, the higher the dissolving capacity of the solvent. The polymer concentration at which the LC phase is formed in the system also increases with a reduction in the acceptor number characterizing the acidity of the solvent. A lower acidity provides an easier donation of electrons to the acceptor compound (cellulose ether molecules). The tendency toward increase in the dissolving capacity of solvent with an increase in polarity is also observed, but it is not monotonic. These results confirm the concept of electron-donor–acceptor interaction proposed for cellulose solutions [27]. The studied cellulose derivatives exhibit stronger donor properties than the acceptor ones.

CONCLUSIONS

It has been shown that, as the molecular mass of cellulose ether increases, the boundary curve separating the isotropic region from the anisotropic one on the phase diagram shifts to the region of higher temperatures and lower concentrations of the polymer. Thus, the systems with LC transitions follow the same dependence as the systems with crystalline phase separations [46]; that is, with the rise in the molecular mass of the crystallizing polymer, the liquidus curve also shifts to lower concentrations of the polymer and higher temperatures.

The replacement of the hydroxypropyl radical in cellulose ether units with ethyl or hydroxyethyl radicals leads to a decrease in the concentration of LC phase formation owing to the facilitated interaction between the units of neighboring macromolecules. The introduction of nitro groups into the units of CEC chains increases the rigidity of chains; as a result, the degree of asymmetry of macromolecules grows; therefore, the LC phase is formed at lower concentrations of the polymer.

As was found for several cellulose ether–solvent systems, the higher the polarity of solvent molecules (the higher the dipole moment of the molecule), the more negative the Gibbs energy of mixing and the higher the second virial coefficients, that is, the better the interaction between the components. Thus, in a first approximation, the dipole moment can be used as an estimate of solvent quality for cellulose ethers. The results of this study make it possible to refine the concept of electron donor–acceptor interaction proposed for cellulose ether solutions [27]

REFERENCES

1. V. G. Kulichikhin and L. K. Golova, Khim. Drev., No. 3, 9 (1985).
2. *Orientation Phenomena in Polymer Solutions and Melts,* Ed. by A. Ya. Malkin and S. P. Papkov (Khimiya, Moscow, 1980) [in Russian].
3. S. P. Papkov and V. G. Kulichikhin, *Liquid Crystalline State of Polymers* (Khimiya, Moscow, 1977) [in Russian].
4. A. P. Kapustin, *Experimental Methods for Investigation of Liquid Crystals* (Nauka, Moscow, 1978) [in Russian].
5. *Liquid Crystal Polymers,* Ed. by N. A. Platé (Khimiya, Moscow, 1988) [in Russian].
6. P. G. De Gennes, *The Physics of Liquid Crystals* (Cambridge Univ. Press, London, 1974).
7. *Liquid Crystalline Order in Polymers,* Ed. by A. Blumstein (Academic, New York, 1978).

8. *Liquid Crystals,* Ed. by S. I. Zhdanov (Khimiya, Moscow, 1979) [in Russian].
9. N. A. Platé and V. P. Shibaev, *Comb-Shaped Polymers and Liquid Crystals* (Mir, Moscow, 1981) [in Russian].
10. A. P. Filippov, Polym. Sci., Ser. B **46** (1), 66 (2004).
11. V. A. Kargin and G. L. Slonimskii, Zh. Fiz. Khim. **15** (9), 1022 (1941).
12. R. Werbowij and D. Gray, Macromolecules **13** (1), 261 (1980).
13. G. Conio, E. Bianchi, A. Ciferri, A. Tealdi, and M. A. Aden, Macromolecules **16** (8), 1264 (1983).
14. F. Fried, J. M. Gilli, and P. Sixou, Mol. Cryst. Liq. Cryst. **98** (1–4), 209 (1983).
15. N. G. Bel'nikevich, L. S. Bolotnikova, L. I. Kutsenko, Yu. N. Panov, and S. Ya. Frenkel', Vysokomol. Soedin., Ser. B **27** (5), 332 (1985).
16. P. Navard, I. M. Haudin, and D. G. Dayan, Macromolecules **14** (6), 715 (1981).
17. B. Nystrom and R. Bergman, Eur. Polym. J. **14** (6), 431 (1978).
18. G. H. Meeten and P. Navard, Polymer **23** (12), 1727 (1982).
19. R. S. Werbowyj and D. G. Gray, Mol. Cryst. Liq. Cryst. **34** (4), 97 (1976).
20. R. S. Werbowyj and D. G. Gray, Polym. Prepr. (Am. Chem. Soc., Div. Polym. Chem.) **20** (1), 102 (1979).
21. R. S. Werbowyj and D. G. Gray, Macromolecules **13** (1), 69 (1980).
22. B. Yu. Yunusov, O. A. Khanchich, A. K. Dibrova, M. T. Primkulova, and A. T. Serkov, Vysokomol. Soedin., Ser. B **24** (6), 414 (1982).
23. M. M. Iovleva, Vysokomol. Soedin., Ser. A **31** (4), 808 (1989).
24. K. Shimura, J. L. White, and J. F. Feller, J. Appl. Polym. Sci. **26** (7), 2165 (1981).
25. G. Charlet and D. G. Gray, Macromolecules **20** (1), 33 (1987).
26. S. Fortin and G. Charlet, Macromolecules **22** (5), 2286 (1989).
27. L. K. Golova, V. G. Kulichikhin, and S. P. Papkov, Vysokomol. Soedin., Ser. A **28** (9), 1795 (1986).
28. S. A. Vshivkov and E. V. Rusinova, Polym. Sci., Ser. A **50** (7), 725 (2008).
29. S. A. Vshivkov and A. G. Galyas, Izv. Vyssh. Uchebn. Zaved., Khim. Khim. Tekhnol. **51** (5), 78 (2008).
30. S. A. Vshivkov, E. V. Rusinova, and A. G. Galyas, Eur. Polym. J. **59** (8), 326 (2014).
31. S. A. Vshivkov, *Thermodynamics. Physical Chemistry of Aqueous Systems* (In Tech, Croatia, 2011), p. 407.
32. S. A. Vshivkov and T. S. Soliman, Polym. Sci., Ser. A **58** (4), 499 (2016).
33. S. A. Vshivkov and A. A. Byzov, Polym. Sci., Ser. A **55** (2), 102 (2013).
34. Y. Nichio, R. Chiba, Y. Miyashita, K. Oshima, T. Miyajima, N. Kimura, and H. Suzuki, Polym. J. **34** (9), 149 (2002).
35. S. A. Vshivkov, E. V. Rusinova, and L. I. Kutsenko, Polym. Sci., Ser. B **49** (5–6), 114 (2007).
36. S. A. Vshivkov and T. S. Soliman, Polym. Sci., Ser. A **58** (3), 307 (2016).
37. L. I. Kutsenko, L. M. Kalyuzhnaya, E. B. Karetnikova, G. A. Petropavlovskii, and S. Ya. Frenkel', Zh. Prikl. Khim. **66** (2), 386 (1993).
38. L. M. Kalyuzhnaya, L. I. Kutsenko, E. B. Karetnikova, E. N. Vlasova, and A. M. Bochek, Russ. J. Appl. Chem. **79** (9), 1500 (2006).
39. S. A. Vshivkov, L. V. Adamova, E. V. Rusinova, A. P. Safronov, V. E. Dreval', and A. G. Galyas, Polym. Sci., Ser. A **49** (5), 578 (2007).
40. S. A. Vshivkov, E. V. Rusinova, N. V. Kudrevatykh, A. G. Galyas, M. S. Alekseeva, and D. K. Kuznetsov, Polym. Sci., Ser. A **48** (10), 1115 (2006).
41. P. J. Flory, Proc. R. Soc. London, Ser. A **234** (1), 73 (1956).
42. S. V. Troshenkova, E. S. Sashina, and N. P. Novoselov, Russ. J. Gen. Chem. **80** (3), 501 (2010).
43. S. A. Vshivkov, A. G. Galyas, L. I. Kutsenko, I. S. Tyukova, T. V. Terziyan, and A. V. Shepetun, Polym. Sci., Ser. A **53** (1), 1 (2011).
44. S. A. Vshivkov and A. G. Galyas, Polym. Sci., Ser. A **53** (11), 1032 (2011).
45. S. A. Vshivkov, L. V. Adamova, and B. I. Lirova, Polym. Sci., A **54** (11), 821 (2012).
46. S. A. Vshivkov, *Phase Transitions of Polymer Systems in External Fields* (Izd-vo Lan', St. Petersburg, 2013) [in Russian].
47. H. Fisher, M. Murray, A. Keller, and J. A. Odell, J. Mater. Sci. **30** (18), 4623 (1995).
48. V. P. Belousov and M. Yu. Panov, *Thermodynamics of Nonelectrolyte Aqueous Solutions* (Khimiya, Leningrad, 1983) [in Russian].
49. K. Kamide, M. Saito, and T. Abe, Polym. J. **13** (5), 421 (1981).
50. *Chemist Handbook* (Khimiya, Leningrad, 1966), Vol. 1 [in Russian].
51. A. A. Tager, *Foundations on Noneletrolyte Solutions* (Izd-vo Ural'skogo Univ., Yekaterinburg, 1993) [in Russian].
52. K. Burger, *Experimental Methods for Investigation of Solvation, Ionic and Complex Formation Reactions in Nonaqueous Solutions* (Akademiai Klado, Budapest, 1982).

Translated by K. Aleksanyan